SYNCELL

WHITE PAPER

Unveiling Primary Ciliary Proteins with Microscoop®

Authors

Hsiao-Jen Chang, Chantal Hoi Yin Cheung, and Hsuan-Hsuan Lu

Introduction

Primary cilia are microtubule-based organelles extending from the surface of most mammalian cells, playing pivotal roles in signal transduction and cellular functions[1]. Malfunctions of primary cilia are implicated in a number of genetic disorders termed ciliopathies, including polycystic kidney disease[2], Bardet-Biedl syndrome[3], and Joubert syndrome[4]. These conditions adversely affect organs such as the kidneys, retina, and brain, influencing key biological processes like cell cycle regulation and tissue development. The study of primary cilia, despite their significance, is filled with challenges. The organelles' diminutive size and structural delicacy significantly complicate their analysis. Additionally, the dynamic nature of their assembly further complicates their study, necessitating high-resolution techniques for detailed analysis.

Addressing these challenges, the Microscoop® platform emerges as an advancement in biological research technology, particularly enhancing the capability for spatial photolabeling at the microscale. It enables the in-depth investigation of primary cilia, providing the necessary precision and detail to comprehensively explore their biological function. With the potential to transform our understanding of ciliary functions in both health and disease, its application in proteomic analysis demonstrates its utility in unraveling the complex protein constitutes of primary cilia, essential for elucidating cellular mechanisms and pathogenesis.

Capturing and analyzing primary cilia with Microscoop®

The Microscoop® platform is designed for the isolation and identification of proteins within submicron cellular regions, specifically aiming to target and analyze subcellular organelles such as primary cilia. It combines a motorized epifluorescence microscope, a high-resolution sCMOS camera, and a two-photon light source. This system is further enhanced by a specially developed photochemical probe (Fig. 1), allowing for precise targeting and isolation of primary cilia for proteomic analysis. To facilitate visualization, primary cilia are pre-stained with the well-known marker polyglutamylation modification (GT335). Real-time image analysis is employed to segment the primary cilia and filter out non-specific signals, using a combination of thresholding, size and length exclusion, and morphological recognition techniques. This ensures efficient segmentation of each Field of View (FOV) image for identifying primary cilia, thereby enabling effective path planning and labeling control. Through the use of two-photon illumination, the system triggers photochemical agents to photo-biotinylate proteins within the primary cilia. The Microscoop® platform controls the sequential photo-biotinylation of individual primary cilia via mechatronic position control, processing millions of primary cilia to collect sufficient proteins for downstream proteomic analysis. The photo-biotinylated proteins are then subjected to streptavidin pull-down, followed by hypothesis-free mass spectrometry (LC-MS/MS) analysis, facilitating a comprehensive proteomics discovery. By integrating ultrahigh-content, high-speed microscopy with targeted photo-biotinylation, the Microscoop® platform revolutionizes the study of primary cilia, enabling spatial isolation for proteomic discovery.

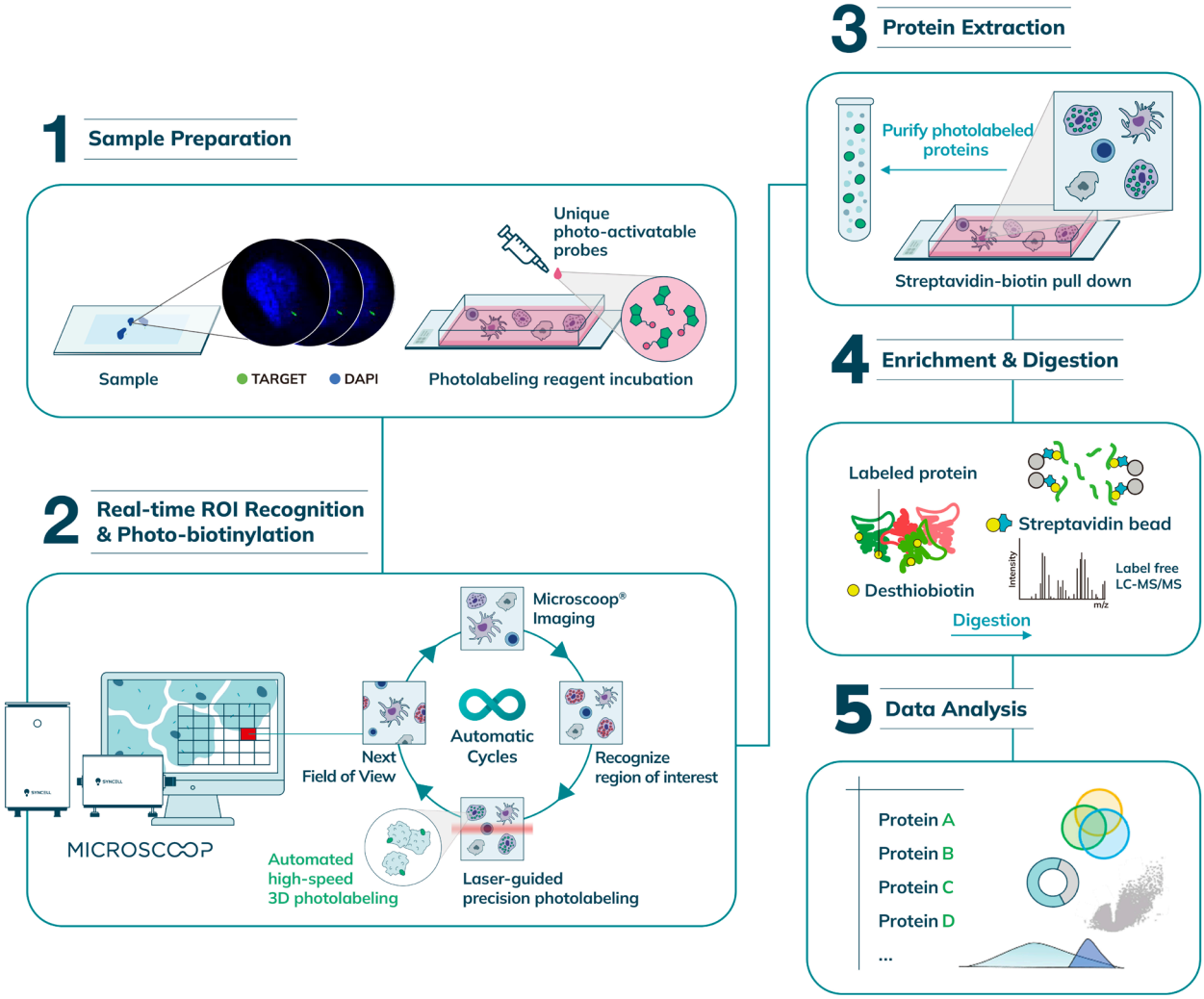

Fig. 1 | Schematic workflow for mapping the primary cilia proteome. A microscopy-guided protein discovery platform integrates image acquisition, photochemistry, microscopy, optics, and mechatronics enables ultrahigh-content *in situ* photolabeling followed by mass spectrometry analysis.

Microscoop® has been engineered to enable photolabeling at the subcellular level, targeting ROIs such as primary cilia, which are presumed to have uniform protein constituents identifiable by distinct morphological features and contrast under microscopy. This method involves several steps executed millions of times: 1) employing microscopy to identify primary cilia; 2) capturing images; 3) processing images to eliminate background noise; 4) recognizing primary cilia patterns; 5) illuminating within primary cilia for photochemical labeling; 6) transitioning to the next FOV (Fig. 2). This repetitive process is crucial for spatially isolating proteins, thereby gathering enough proteins to address the challenge of protein amplification. Remarkably, existing technologies lack the capability for such extensive and rapid repetition across locations and timespans.

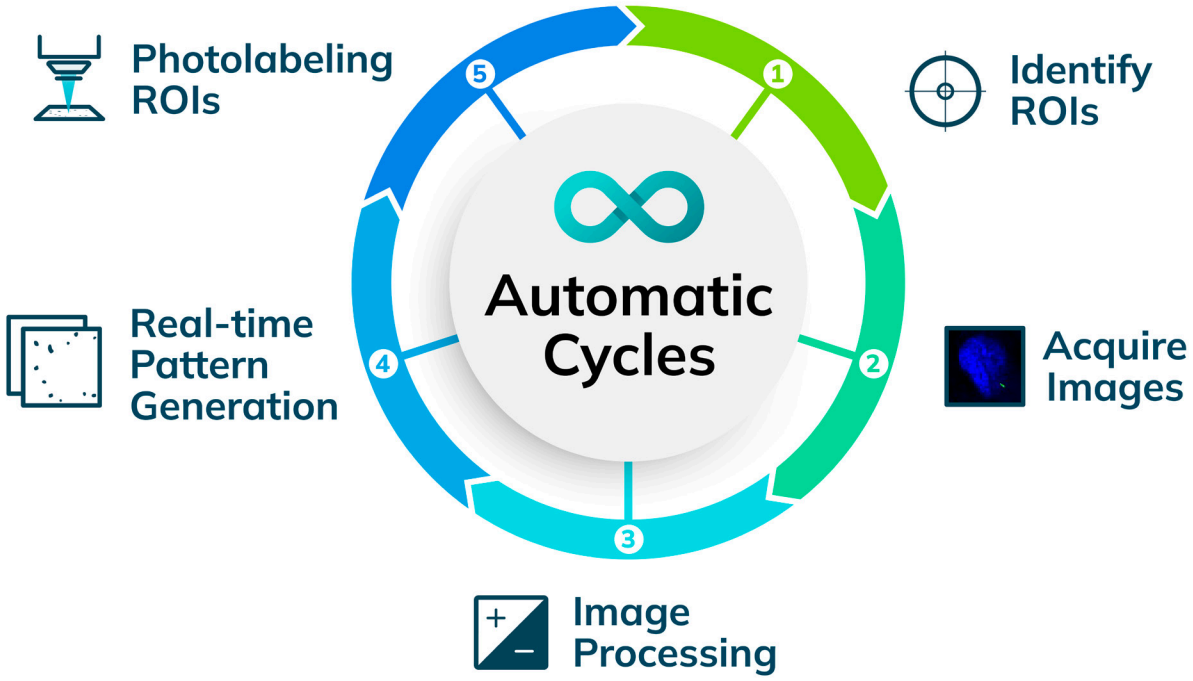

Fig. 2 | The process and design of the microscopy-guided protein lisolation platform. The process includes: (1) identifying the primary cilia by light microscopy; (2) acquiring images of primary cilia; (3) processing images to identify primary cilia as ROIs; (4) generating realtime patterns of ROIs; (5) illuminating the selected region within ROIs for protein photo-biotinylation; (6) moving the stage to the next FOV; and repeating steps 1-5 for each FOV until all FOVs of intereest have been processed.

The images are processed in real-time to segment the primary cilia using image processing techniques, including thresholding, filtering, size and length exclusion, and morphological recognition. These steps are uniformly applied across all FOVs, with pre-processing or post-processing adjustments to ensure consistent image quality. The segmentation results, depicted in Figure 3, require 0.1 to 1 second for completion, varying with the image's complexity and quality. Following segmentation, the coordinates of the primary cilia's grid points are determined. A planned path for photochemical activation is then optimized and used to guide the galvanometers (galvos) across these points. The galvos and the Acousto-Optic Modulator (AOM) synchronize to within approximately 100 microseconds, enabling precise control over the locations and duration, thus ensuring a consistent photochemical reaction across all spots. For locations with multiple primary cilia, the scanning path sequentially targets each cilium, initiating at the periphery and spiraling clockwise towards the center before proceeding to the next cilium's starting point. This method reduces travel time and minimizes mechanical stress on the galvos. Achieving this level of intricacy within a feasible timeframe relies on speed optimization, seamless automation, and accurate mechatronic control throughout the process.

To validate the labeling accuracy and precision for primary cilia as small as 0.2 μm in width and 1 μm in length, primary cilia of RPE-1 cells were pre-stained with GT335, followed by photo-biotinylation using Microscoop®. The platform accurately recognized primary cilia, enabling targeted spatial photolabeling with two-photon illumination. This method facilitated the isolation of primary cilia proteins with high specificity, as demonstrated by the congruence between the *in situ* biotinylated regions (green) and the primary cilia (red) fluorescence in both lateral (xy) and axial (z) directions (Fig. 3, right panel).

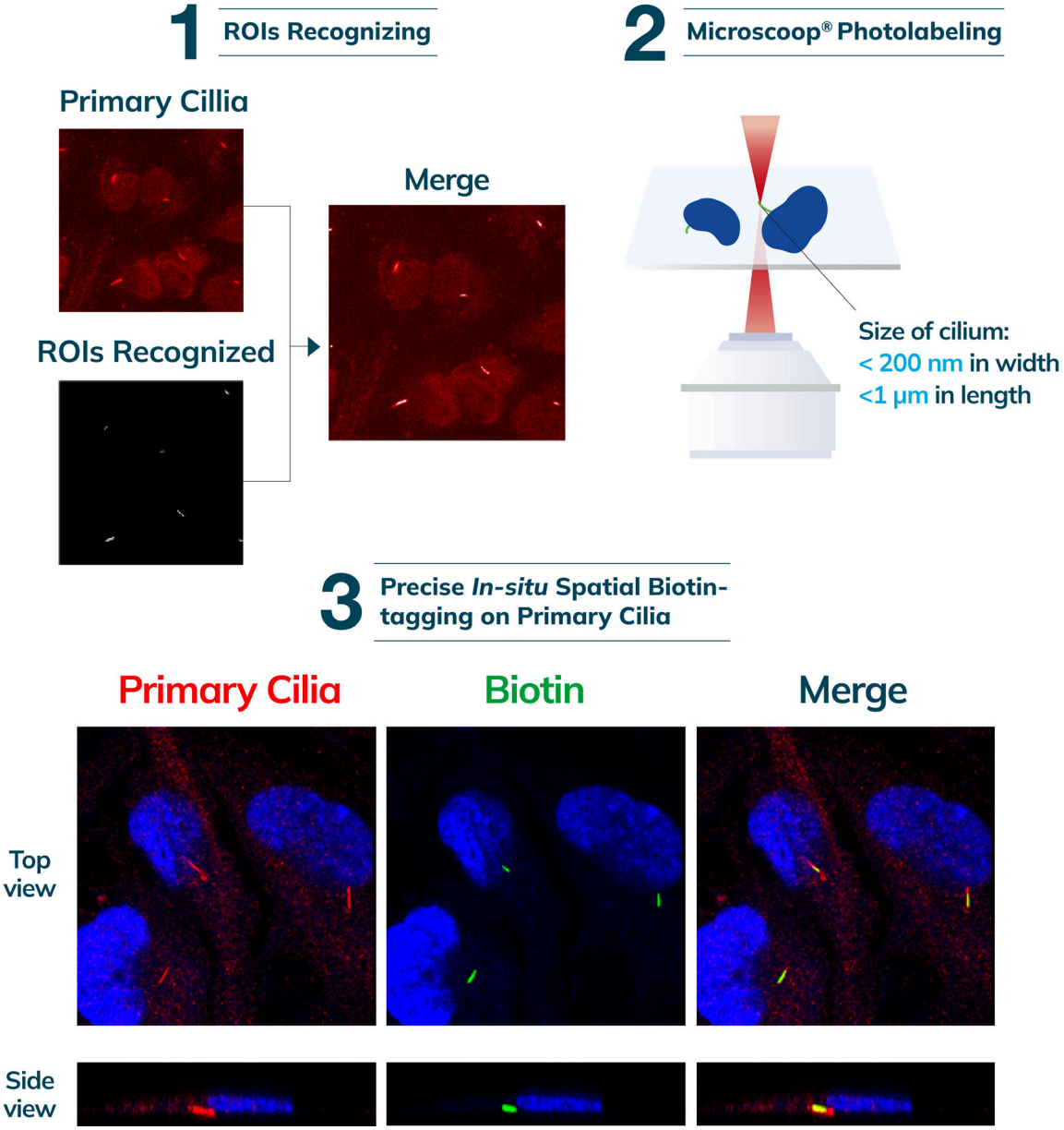

Fig. 3 | Primary cilia are processed by filtering and segmentation by image processing (left), Confocal micrographs depicting precise and accurate photolabeled primary cilia at lateral (xy)- and axial (z) directions (right). Red: GT335, Green: NeutrAvidin-488, Blue: DAPI.

Unveiling ciliary proteins andfunctional insights

Photolabeling experiments were conducted on PFA fixed RPE-1 cells, specifically targeting regions marked with GT335 to elucidate the protein composition of primary cilia (Fig. 4A). Following hours of precise photolabeling, cells were harvested and lysed to extract proteins. The photolabeled proteins were subsequently enriched through streptavidin bead pulldown, digested with trypsin, and analyzed via LC-MS/MS. This comprehensive analysis resulted in the high-confidence identification of 4,233 proteins (Fig. 4B) and a total of 608 ciliary proteins were identified among experiments (Fig. 4C). Among the identified proteins, key ciliary trafficking components such as intraflagellar transport proteins (IFTs), kinesins, dyneins, GTPases, and phosphatidylinositol phosphates (PIPs) were enriched, exhibiting high photolabeling to control (PL/CTL) ratios (Fig. 4D). Additionally,

proteins involved in structural support and cellular organization, including microtubules, septins, and annexins, were also observed to be enriched within the photolabeled sample.

A

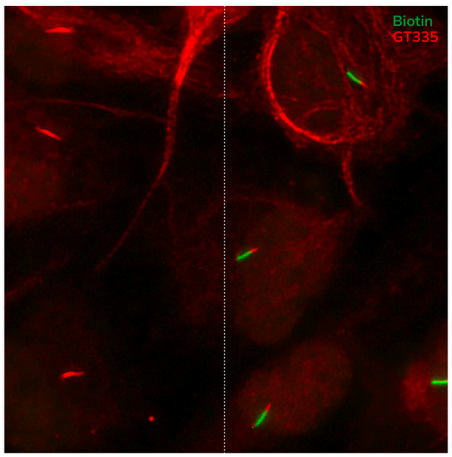

B

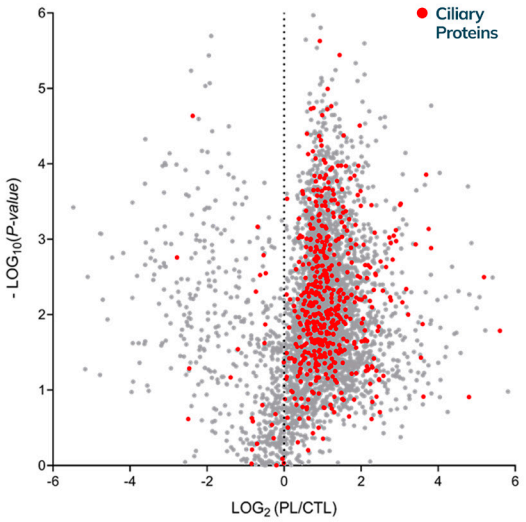

C

Photo-biotinylation Enriched Primary Cilia Proteins

ABCC4	ATG3	CEP112	CTTN	ELMO2	HSPA4L	KIF23	MYO1E	PCM1	QKI	SDCCAG8	TNS3	WDHD1
ABLIM1	ATG5	CEP120	CUL3	ELP4	HSPA5	KIF24	MYO1F	PCNT	RAB10	SEC23A	TOGARAM2	WDR1
ABRAXAS2	ATG7	CEP128	CYFIP2	EML1	HSPA8	KIF2A	MYO3B	PDCD6IP	RAB11A	SEC63	TP53BP1	WDR11
ACLY	ATP1A1	CEP131	CYLD	EPB41L3	HSPBP1	KIF2C	MYO5A	PDE1C	RAB13	SEPTIN10	TPM3	WDR12
ACOT9	ATP1B1	CEP135	CYP51A1	EPS15	HSPD1	KIF3A	MYO5C	PDGFRA	RAB14	SEPTIN11	TRABD	WDR13
ACTN1	ATP2A2	CEP152	DCTN1	EPS8L2	HUWE1	KIF3B	MYO6	PDIA6	RAB18	SEPTIN2	TRAPPC10	WDR18
ACTN4	ATP2B4	CEP164	DCTN2	ERC1	HYDIN	KIF4A	MYO9A	PDXDC1	RAB1B	SEPTIN6	TRAPPC3	WDR19
ACTR1A	ATP6V0D1	CEP170	DCTN3	EXOC3	HYOU1	KIF5B	MYO9B	PEX6	RAB21	SEPTIN7	TRAPPC9	WDR24
ACTR2	ATP6V1A	CEP170B	DCTN4	EXOC4	IDE	KIF5C	MYOF	PFKM	RAB23	SEPTIN8	TRIM32	WDR26
ACTR3	ATP6V1D	CEP192	DDX1	EXOC5	IFIT3	KIF7	NAXE	PFN2	RAB2A	SEPTIN9	TRIM59	WDR3
ADCY3	ATXN10	CEP250	DDX21	EXOC6	IFT122	KIFAP3	NBEA	PIBF1	RAB32	SETX	TRIP11	WDR33
ADD3	ATXN2L	CEP290	DDX56	EXOC6B	IFT140	KIFBP	NCAPD2	PIGS	RAB34	SF3A1	TSC2	WDR35
AK1	AURKA	CEP350	DDX6	EZR	IFT172	KIFC1	NCAPG	PIK3C3	RAB35	SF3B2	TSG101	WDR36
AK2	AXL	CEP43	DHX30	FHL2	IFT27	KIFC3	NDC80	PIK3R4	RAB3B	SH3GL1	TTC21B	WDR37
AKAP9	BBS1	CEP44	DHX9	FKBP5	IFT52	KIRREL1	NDE1	PIN1	RAB3C	SHROOM3	TTF2	WDR4
AKT1	BBS2	CEP57	DLD	FKBP8	IFT56	LAMA5	NEDD1	PJA2	RAB5A	SKP1	TTLL12	WDR43
ALMS1	BBS4	CEP63	DLG5	FLNA	IFT57	LDHB	NEDD4L	PKD2	RAB5B	SLAIN2	TUBA1B	WDR45
ANKMY2	BBS7	CEP76	DMD	FNBP1L	IFT70A	LGALS3	NEK1	PKM	RAB5C	SLIRP	TUBA4A	WDR46
ANKS3	BBS9	CEP78	DNAAF5	FOCAD	IFT74	LRBA	NEK6	PLK1	RAB6A	SLK	TUBA4B	WDR47
ANXA1	BRI3BP	CEP83	DNAH11	GAK	IFT80	MACF1	NEK9	POLA2	RAB7A	SMARCA4	TUBB	WDR48
ANXA11	BSG	CEP89	DNAJA1	GANAB	IFT81	MAP1A	NHERF1	POLD1	RAB8A	SMPD4	TUBB2A	WDR5
ANXA6	C2CD3	CEP97	DNAJB1	GDI2	IFT88	MAP1B	NID2	POR	RAB8B	SORD	TUBB3	WDR55
ANXA7	CALR	CFAP20	DNM2	GLE1	IMPDH2	MAP1S	NIN	PPA1	RABEP2	SPTAN1	TUBB4A	WDR6
AP2A1	CALU	CHD4	DNMT1	GLOD4	INPP4A	MAP4	NME7	PPIA	RABL3	SQSTM1	TUBB4B	WDR62
AP3M2	CAMK2D	CHORDC1	DPYSL2	GLRX3	INPP4B	MAP4K3	NOL6	PPID	RABL6	SRI	TUBB6	WDR7
APEX1	CAMSAP1	CIT	DROSHA	GMDS	INPP5F	MAP9	NOTCH2	PPP1CC	RAC1	SRR	TUBGCP2	WDR70
APP	CAMSAP2	CKAP2	DSG2	GNA11	INPPL1	MAPKAP1	NPHP3	PPP2R1A	RAN	SSX2IP	TUBGCP3	WDR75
APPL1	CAPN1	CKAP5	DSTN	GOT2	INTS1	MAPKBP1	NPHP4	PRDX4	RANBP1	STAT3	TUBGCP4	WDR77
ARF4	CAPN2	CLASP1	DYNC1H1	GPI	INTS2	MAPRE1	NR3C1	PRIM1	RANGAP1	STIP1	TUBGCP6	WDR81
ARFGEF2	CAPZB	CLIC1	DYNC1I2	GRK2	IPO5	MDC1	NUDC	PRKAA1	RAPGEF2	STK33	TXNIP	WDR82
ARHGAP1	CARS1	CLTB	DYNC2H1	GSK3B	IQCE	MDM1	NUP210	PRKAR1A	RBM22	SUPT5H	TXNL1	WDR90
ARHGAP29	CASK	CLTC	DYNC2I1	GSN	ITGA3	MED16	NUP214	PRKAR2A	RHOT1	SURF4	UBA1	WDR91
ARHGAP35	CAV1	CLUAP1	EEF1A1	HAT1	JPT2	MICAL3	NUP35	PRKAR2B	RICTOR	SYNE1	UBA6	WIZ
ARHGEF18	CBL	CNOT10	EFCAB7	HAUS1	KATNAL1	MLEC	NUP37	PRKCA	RO60	SYNE2	UBAP2L	WRAP73
ARL13B	CC2D2A	CNTRL	EFHC1	HAUS3	KATNAL2	MPDU1	NUP62	PRKD2	RPA1	TAGLN2	UBE3C	YTHDF3
ARL14EP	CCDC191	COL18A1	EFTUD2	HAUS4	KATNB1	MROH2B	NUP93	PSMB4	RPGRIP1L	TAPT1	UBE4B	YWHAE
ARL2	CCDC61	COPG1	EGFR	HAUS5	KDM3B	MSN	OCRL	PSMC2	RPL9	TARS1	UGGT1	YWHAG
ARL3	CCDC88A	COPG2	EHD1	HAUS6	KHSRP	MTCL1	ODF2	PSMC3	RPS6KA1	TBC1D31	USP9X	YWHAQ
ARL6	CCP110	COPS8	EHD3	HDAC1	KIF11	MXRA8	OFD1	PSMC5	RPTOR	TCHP	VCAN	ZC2HC1A
ARL6IP4	CCT2	CORO1B	EIF2A	HHIP	KIF13A	MYADM	OGFR	PSMD14	RRM1	TCP1	VCL	ZFYVE19
ARL6IP5	CCT3	CROCC	EIF2S1	HK1	KIF13B	MYCBP2	ORC1	PSMD5	RTCA	THBS1	VCP	ZFYVE26
ARL6IP6	CCT4	CSNK1A1	EIF3A	HMGB2	KIF14	MYH10	OSBPL6	PTBP1	RTN4	THOP1	VDAC2	ZNF318
ARL8B	CCT5	CSNK2B	EIF4B	HNRNPLL	KIF16B	MYO10	P4HA1	PTK2	RUVBL1	TIGAR	VDAC3	ZSCAN18
ARMC9	CCT8	CSRP1	EIF4H	HSP90AA1	KIF1B	MYO18A	PACS1	PTPN23	RUVBL2	TJP2	VPS13A	ZWILCH
ASAP1	CDK1	CSTB	EIF5A	HSP90AB1	KIF1C	MYO19	PAFAH1B1	PTPRK	SCCPDH	TMEM231	VPS35	
ASNS	CDK5RAP2	CTNNA1	EIF6	HSP90B1	KIF20A	MYO1B	PAPSS1	PUM1	SCD	TMPO	VTN	
ATG16L1	CENPF	CTNNB1	EIPR1	HSPA4	KIF22	MYO1C	PARD3	PXDN	SCD5	TNPO1	VWA5A	

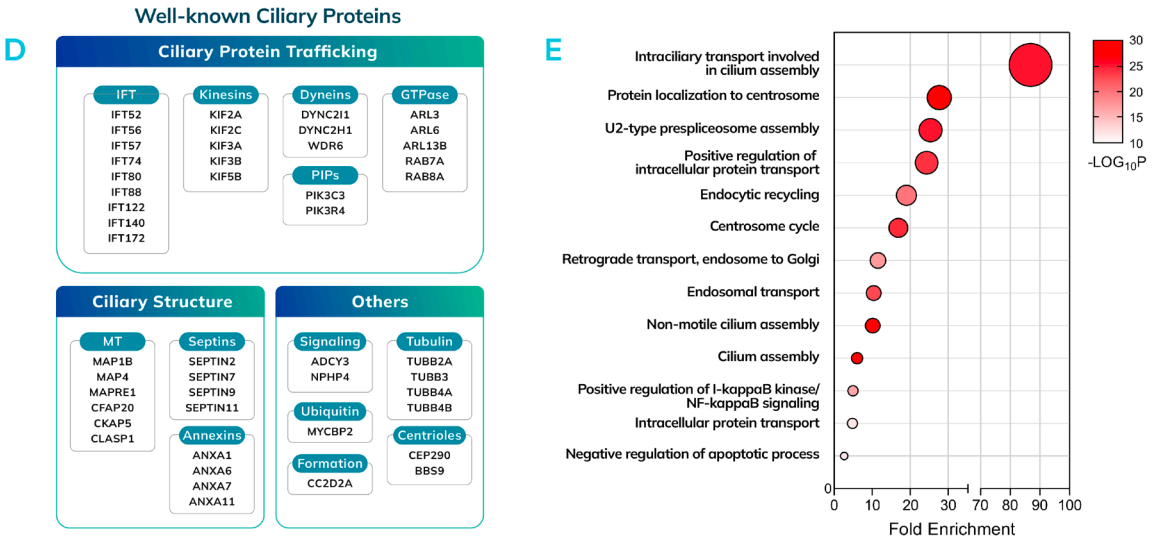

Fig. 4 | (A)Confocal micrographs of unphotolabeled (UL) and photolabeled (PL) at user defined primary cilia. (B)A distribution of overall protein abundances is binned by the ratio of copies in a photolabeled (PL) sample to those in a control (CTL) sample annotated as PL/CTL ratio. Ciliary proteins (red) are enriched in the PL group compared to the CTL sample. (C)608 ciliary proteins identified by Microscoop®. (D)Well-known cilia proteins identified by Microscoop®. (E)The top 100 enriched proteins were subjected to Gene ontology to reveal cilia related biological process.

Gene ontology (GO) enrichment analysis further validated these findings, demonstrating a significant association of the enriched proteins with critical biological processes such as ciliary assembly, transportation, and signaling, underpinning the complex functionality of the ciliary proteome (Fig. 4E). Notably, proteins involved in intraciliary transport, a crucial aspect of cilium assembly, were significantly overrepresented in the GO category related to this process. These findings support the effectiveness of targeted photolabeling and proteomic analysis in revealing the network of proteins essential for ciliary function and structure.

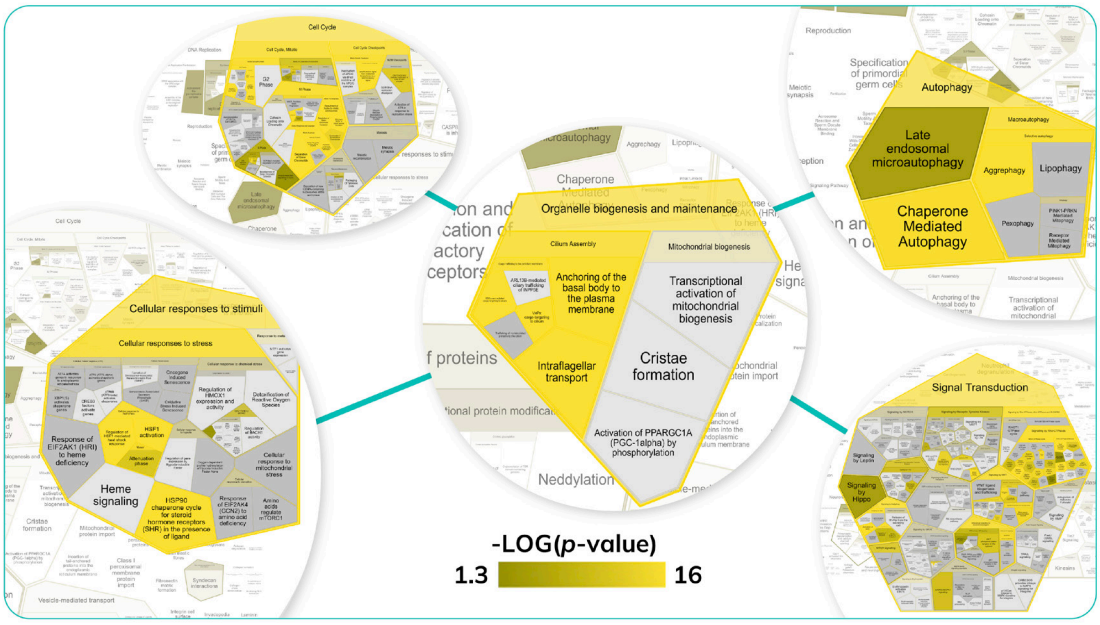

Fig. 5 | 427 enriched ciliary proteins were subjected to Reactome to reveal cilia related pathways.

Furthermore, 427 ciliary proteins showed significant enrichment in the photolabeled group, indicative of their specific association with primary cilia. These 427 known ciliary proteins were subjected to Reactome pathway analysis, revealing major ciliary pathways such as intraflagellar transport, cilium assembly, signal transduction, cellular responses to stimuli and stress, cell cycle regulation, autophagy, and organelle biogenesis and maintenance (Fig. 5). Intraflagellar transport and cilium assembly are essential for the movement of molecular cargo along the cilia, ensuring proper ciliary assembly and function. Signal transduction pathways are critical for cilia in transmitting extracellular signals to the interior, influencing various cellular responses. The involvement of ciliary proteins in the cell cycle highlights the importance of cilia in regulating cell division and growth. Autophagy and organelle biogenesis and maintenance pathways underscore the role of cilia in cellular housekeeping and the recycling of cellular components. These pathways are crucial for ciliary function and development, covering a significant portion of the identified ciliary proteome.

Discovery of novel ciliary proteins

To further explore potential ciliary proteins, we analyzed the top 30 most abundant non-ciliary proteins, referred to as putative ciliary proteins (Fig. 6A). Biological process analysis revealed that these putative ciliary proteins are highly associated with cellular protein localization, protein transport, and regulation of protein stability. These functions are closely related to ciliary activities, suggesting that these proteins may have important roles in ciliary biology (Fig. 6B). Protein-protein interaction network analysis demonstrated that many of these putative ciliary proteins (red circles) interact with the 427 identified ciliary proteins, indicating their potential involvement in ciliary functions (Fig. 6C). These interactions suggest that putative ciliary proteins might participate in crucial processes such as protein trafficking to the cilium, stabilization of ciliary structures, and modulation of ciliary signaling pathways. These findings highlight the significance of these proteins in maintaining the structural and functional integrity of cilia. Moreover, the network analysis revealed specific clusters of interactions where putative ciliary proteins are closely connected with well-known ciliary proteins (black circles). This clustering suggests a coordinated role in ciliary maintenance and function, potentially uncovering new regulatory mechanisms within the cilium. These insights provide a deeper understanding of the protein network dynamics within cilia and highlight the complexity of ciliary protein interactions. However, further experimental validation is necessary to confirm the association of these 30 putative ciliary proteins with primary cilia and to elucidate their precise roles and locations within the ciliary context.

A

Gene Name	Protein Description
PPIB	Peptidyl-prolyl cis-trans isomerase B
ALDH1A3	Retinaldehyde dehydrogenase 3
CAVIN1	Caveolae-associated protein 1
SF3A3	Splicing factor 3A subunit 3
TRIM25	E3 ubiquitin/ISG15 ligase TRIM25
AP2A2	AP-2 complex subunit alpha-2
SRP72	Signal recognition particle subunit SRP72
CTNND1	Catenin delta-1
MARS1	Methionine--tRNA ligase, cytoplasmic
HNRNPDL	Heterogeneous nuclear ribonucleoprotein D-like
PNPLA6	Patatin-like phospholipase domain-containing protein 6
CPNE3	Copine-3
EPHA2	Ephrin type-A receptor 2
SUPT16H	FACT complex subunit SPT16
RPS7	Small ribosomal subunit protein eS7

Gene Name	Protein Description
CD2AP	CD2-associated protein
NUP98	Nuclear pore complex protein Nup98-Nup96
AP3B1	AP-3 complex subunit beta-1
GOLGA4	Golgin subfamily A member 4
CNOT1	CCR4-NOT transcription complex subunit 1
COPB1	Coatomer subunit beta
NPM1	Nucleophosmin
SERPINH1	Serpin H1
UACA	Uveal autoantigen with coiled-coil domains and ankyrin repeats
TKT	Transketolase
AARS1	Alanine--tRNA ligase, cytoplasmic
FLOT2	Flotillin-2
TJP1	Tight junction protein ZO-1
NXF1	Nuclear RNA export factor 1
ARPC1B	Actin-related protein 2/3 complex subunit 1B

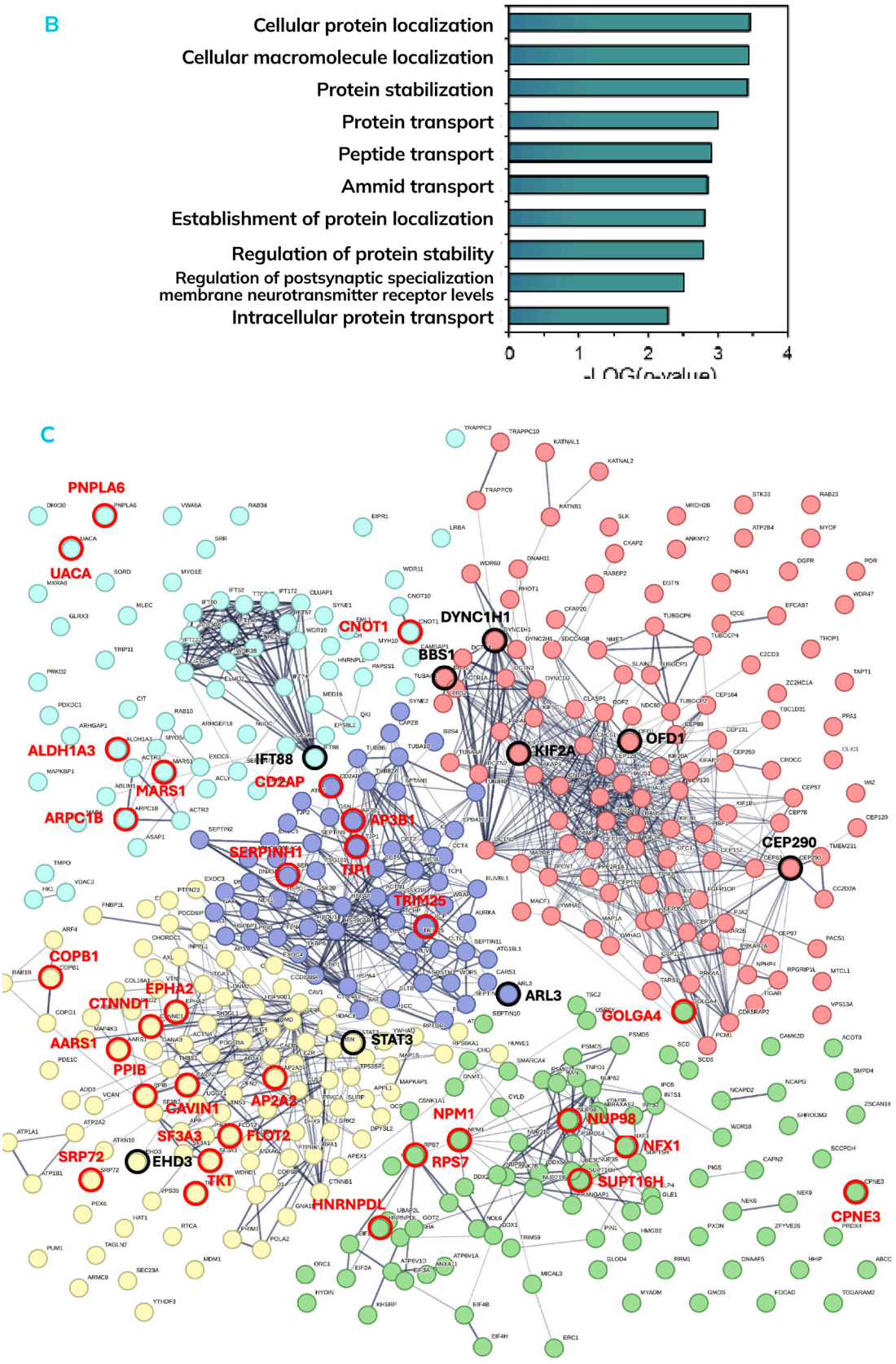

Fig. 6. (A)The list of the top 30 non-ciliary proteins (putative ciliary proteins) enriched by Microscoop®. (B) The top 30 putative ciliary proteins (A) were subjected to Gene ontology to reveal cilia related biological process. (C)The 30 putative ciliary protein and 427 enriched ciliary proteins were subjected to STRING to reveal protein-protein interaction networks, where the 30 putative ciliary proteins are indicated in red and well-known ciliary proteins are indicated in black.

Conclusion

In this white paper, we present a comprehensive exploration of primary cilia, aiming to deepen our understanding of their composition and biological roles. Our research initiated with the precise targeting and labeling of primary cilia utilizing the Microscoop® technology, renowned for its accuracy and specificity in photo-biotinylation within primary cilia. This enabled the provision of a comprehensive list of protein candidates associated with primary cilia.

Our findings demonstrate that the Microscoop® technology effectively enables spatially specific photolabeling of primary cilia, facilitating the identification of both known and novel ciliary proteins and thus enhancing our understanding of this essential cellular component. The total ciliary proteins identified amounted to 608, with significant enrichment of 427 ciliary proteins further analyzed for pathway involvement, revealing key ciliary pathways. The identification of putative ciliary proteins and their interactions with known ciliary proteins opens new avenues for ciliary research, emphasizing the need for further validation studies.

To propel cilia research forward, access to reliable and comprehensive proteomics databases is essential. The currently available open-source cilia databases are fragmented and exhibit inconsistencies, marked by variations in data quality and differences across platforms. This situation, combined with the complexity and small size of primary cilia, presents significant challenges to conducting effective research in this field. In an effort to address these issues, we have collected data from several cilia databases, including Gene Ontology[5], UniProt[6], and CiliaCarta[7], into the Syncell database. The ciliary proteome from Syncell offers a comprehensive and consistent dataset of ciliary proteins, designed to address the current gaps in research. We aim to empower researchers with the necessary tools for advancing our understanding of ciliary functions and mechanisms.

References

1. Satir, P. & Christensen, S.T. Overview of structure and function of mammalian cilia. *Annu Rev Physiol* **69**, 377-400 (2007).
2. Brown, J.M. & Witman, G.B. Cilia and Diseases. *Bioscience* **64**, 1126-1137 (2014).
3. Tobin, J.L. & Beales, P.L. Bardet-Biedl syndrome: beyond the cilium. *Pediatr Nephrol* **22**, 926-936 (2007).
4. Cantagrel, V. et al. Mutations in the cilia gene ARL13B lead to the classical form of Joubert syndrome. *Am J Hum Genet* **83**, 170-179 (2008).
5. Ashburner, M. et al. Gene ontology: tool for the unification of biology. The Gene Ontology Consortium. *Nat Genet* **25**, 25-29 (2000).
6. UniProt, C. UniProt: the Universal Protein Knowledgebase in 2023. *Nucleic Acids Res* **51**, D523-D531 (2023).
7. van Dam, T.J.P. et al. CiliaCarta: An integrated and validated compendium of ciliary genes. *PLoS One* **14**, e0216705 (2019).

For more information, please visit syncell.com

SYNCELL Inc.

Info@syncell.com